

Supporting Information:

Dehydrogenative coupling promoted by copper catalysts: a way to optimise and upgrade bio-alcohols

Nicola Scotti,^a Federica Zaccheria,^a Claudio Evangelisti,^a Rinaldo Psaro^a and Nicoletta Ravasio^{a*}

^a. CNR Institute of Molecular Sciences and Technology, Via Golgi 19, 20133 Milano, Italy, Phone +39 0250314382;

* Corresponding author, email: n.ravasio@istm.cnr.it

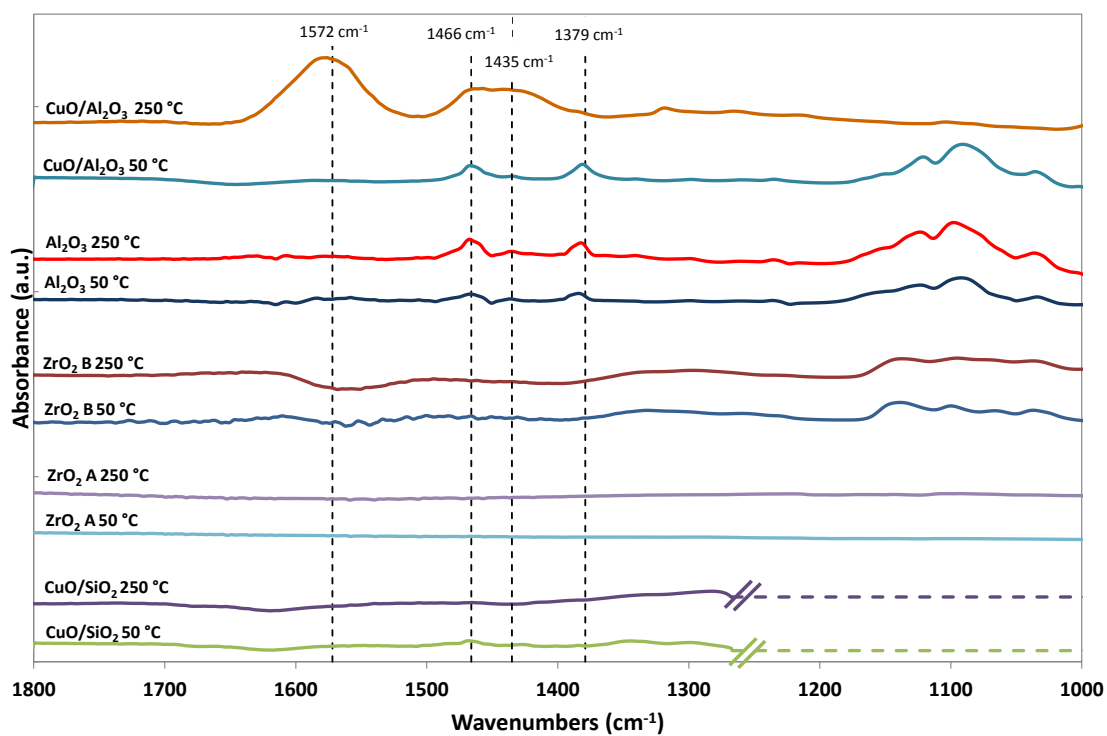
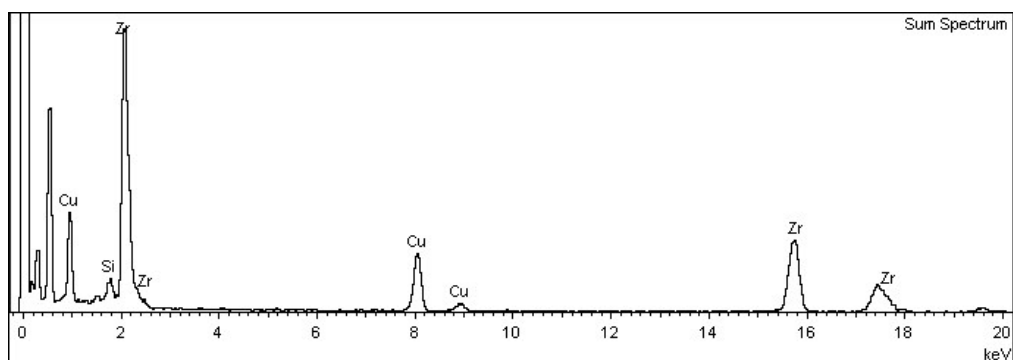


Figure S1. FT-IR of adsorbed 1-butanol over different catalysts and supports



Element	Atomic %	Wt %
Cu	19.3	11.2
Si	8.1	2.1
Zr	72.6	60.5

PM		PA		Atomic %		wt TOT		wt%			wt%	
SiO ₂	60	Si	28.1	Si	8.1	SiO ₂	4.9	SiO ₂	4.4%	→	Si	2.1
ZrO ₂	123	Zr	91.2	Zr	72.6	ZrO ₂	89.3	ZrO ₂	81.6%	→	Zr	60.5
CuO	79,5	Cu	63.5	Cu	19.3	CuO	15.3	CuO	14.0%	→	Cu	11.2
				TOT	100.0	wt tot	109.5					

Figure S2. EDX spectrum of the CuO/ZrO₂ C grain represented in Figure 3. In the tables are reported the Cu, Zr and Si atomic and weight composition and the calculation from atomic% to wt%.

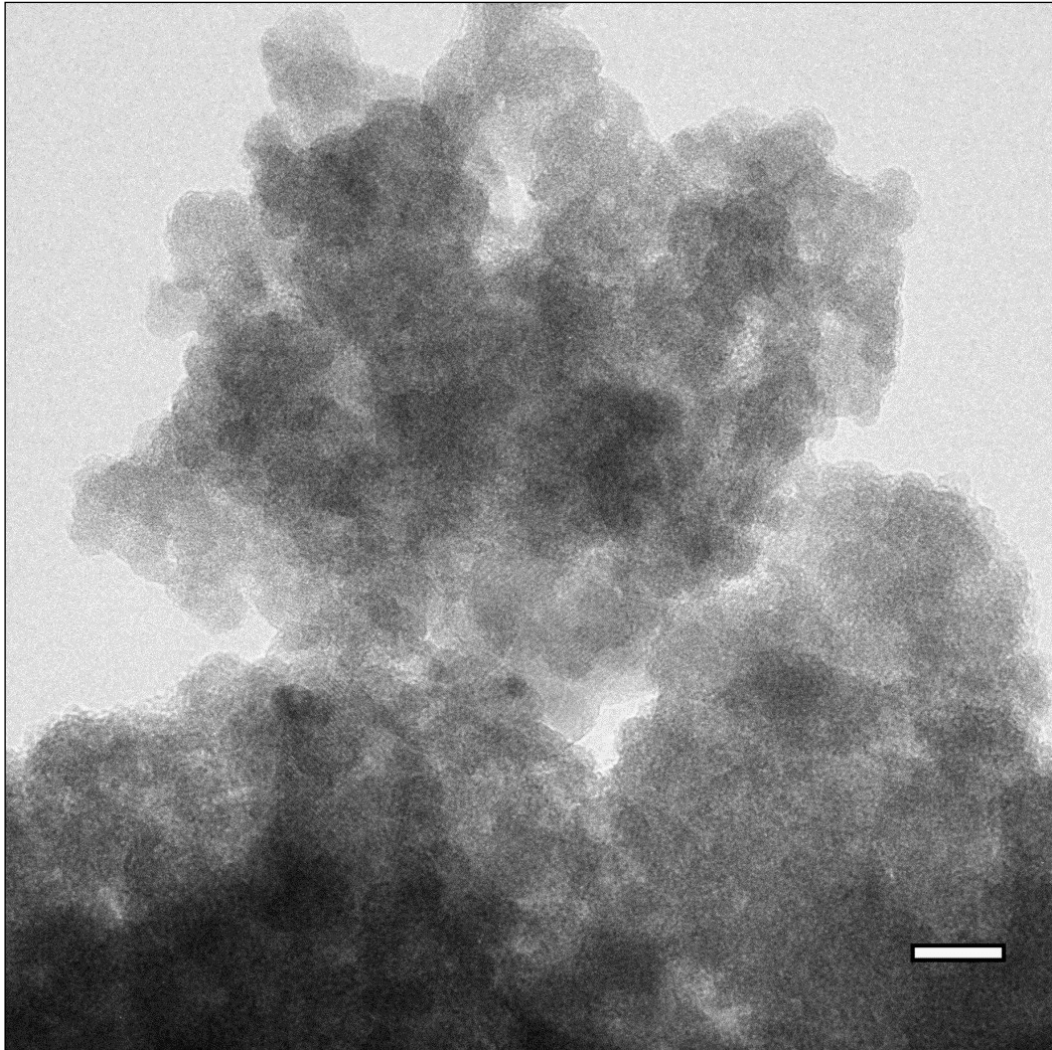


Figure S3. HRTEM micrograph of CuO/ZrO₂ C catalyst.

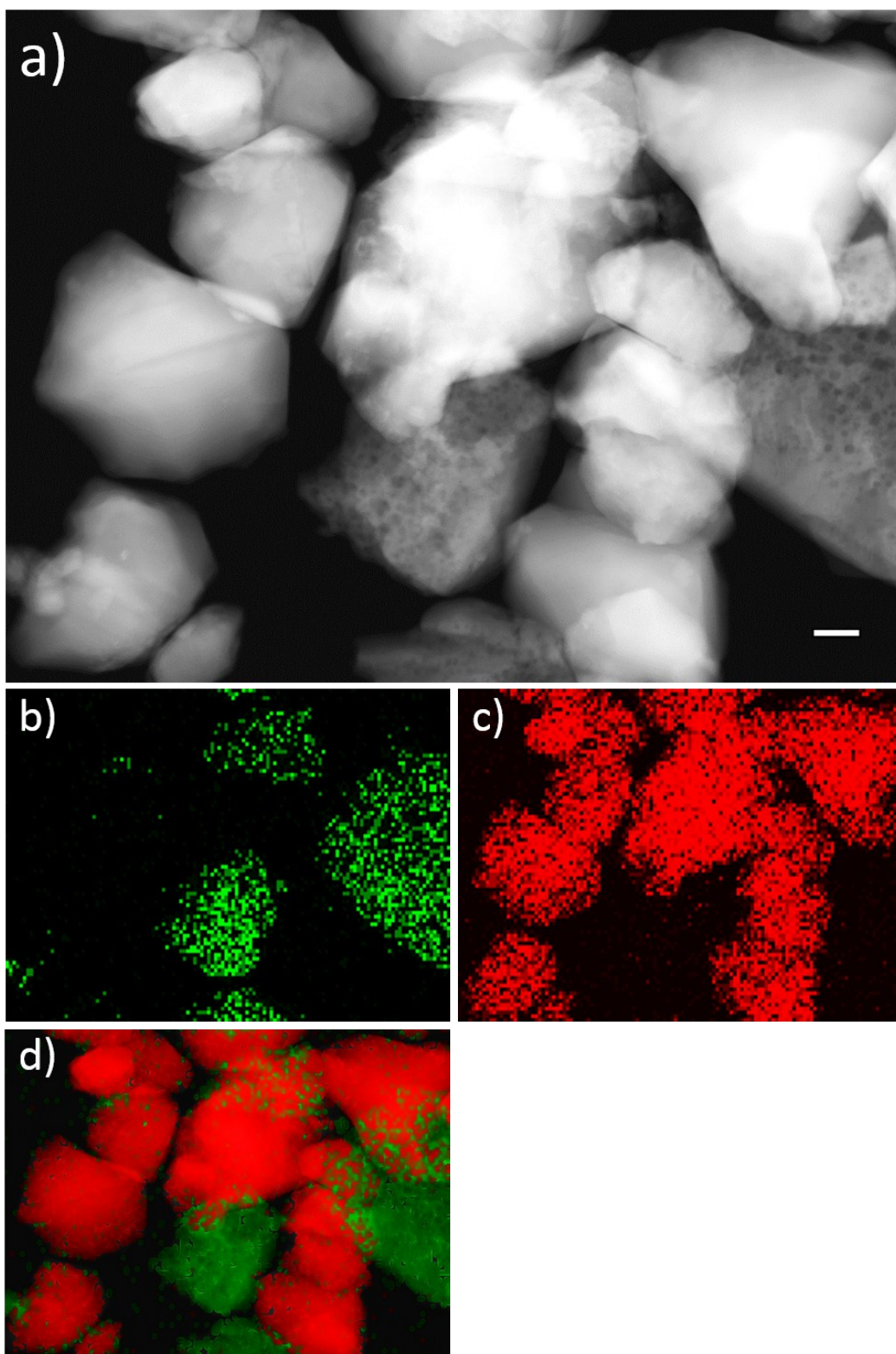


Figure S4. STEM measurements of CuO/ZrO₂. A: a) HAADF image of a catalyst grain (the length of the bar corresponds to 50 nm); b-d) STEM-EDX mapping of the catalyst showing the copper dispersion present in the catalyst: b) copper map (green), c) zirconium map (red), d) overlay of copper (green) and zirconium (red) maps.

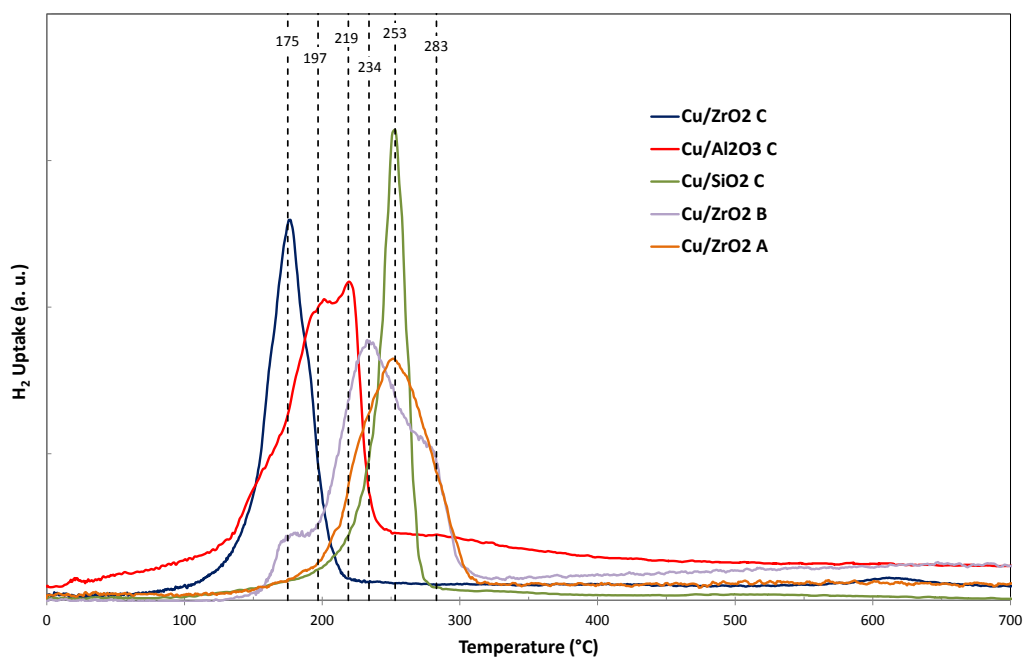


Figure S5.TPR analysis of CuO/ZrO₂ C, CuO/ZrO₂B, CuO/ZrO₂ A, CuO/Al₂O₃ and CuO/SiO₂

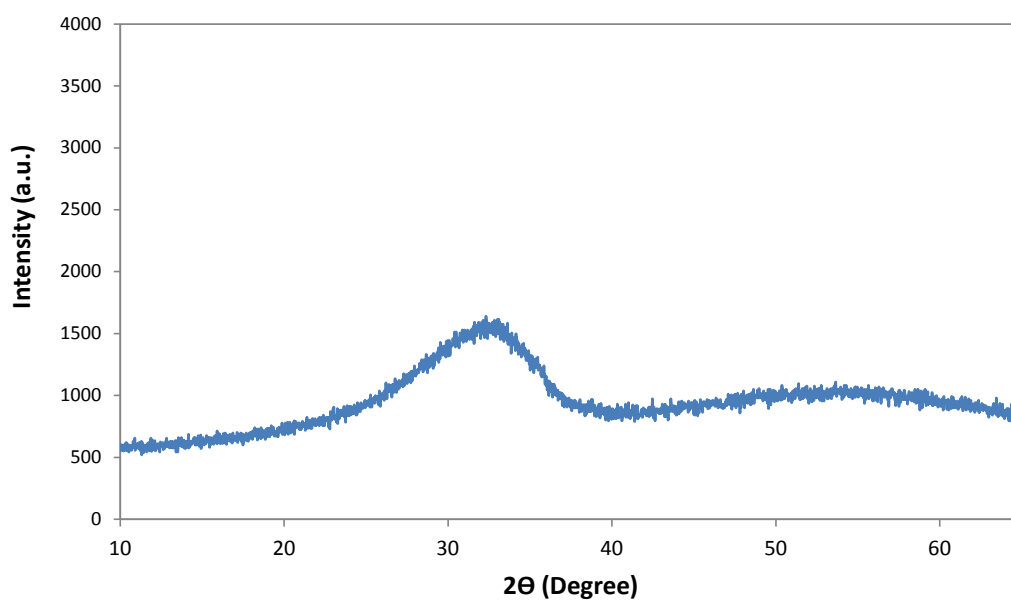


Figure S6. XRD of CuO/ZrO₂ C

Figure S5 shows the XRD pattern for the CuO/ZrO₂ C catalyst. No reflections for the CuO were detected, indicating the high dispersion of the copper phase, while the broad peak is typical of amorphous materials (in the present case the ZrO₂ C phase).

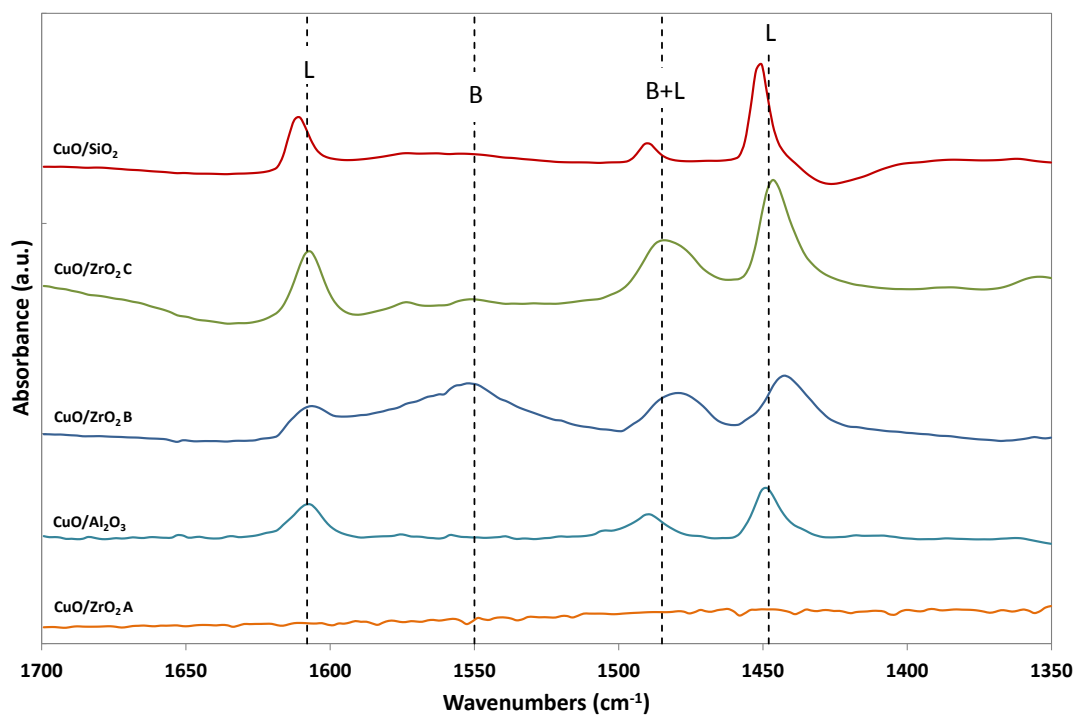


Figure S7. FT-IR of pyridine over different catalysts after degassing at 150 °C

The FT-IR spectrum of pyridine after degassing at 150 °C (Figure S6) shows three main bands at 1446, 1607 and 1485 cm^{-1} , that are in agreement with the presence of Lewis acid sites. For zirconia-based materials the band at 1446 cm^{-1} lies at relative low wavenumbers, very close to the one usually assigned to physisorbed or hydrogen bonded pyridine, but its resistance to outgassing up to 250 °C (together with the bands at 1607 and 1485 cm^{-1}) indicate unambiguously a Lewis acid-base interaction with pyridine. In the case of CuO/ZrO₂ C (very weak) and B a broad band at around 1450 cm^{-1} is typical of the presence of Brønsted acid sites.

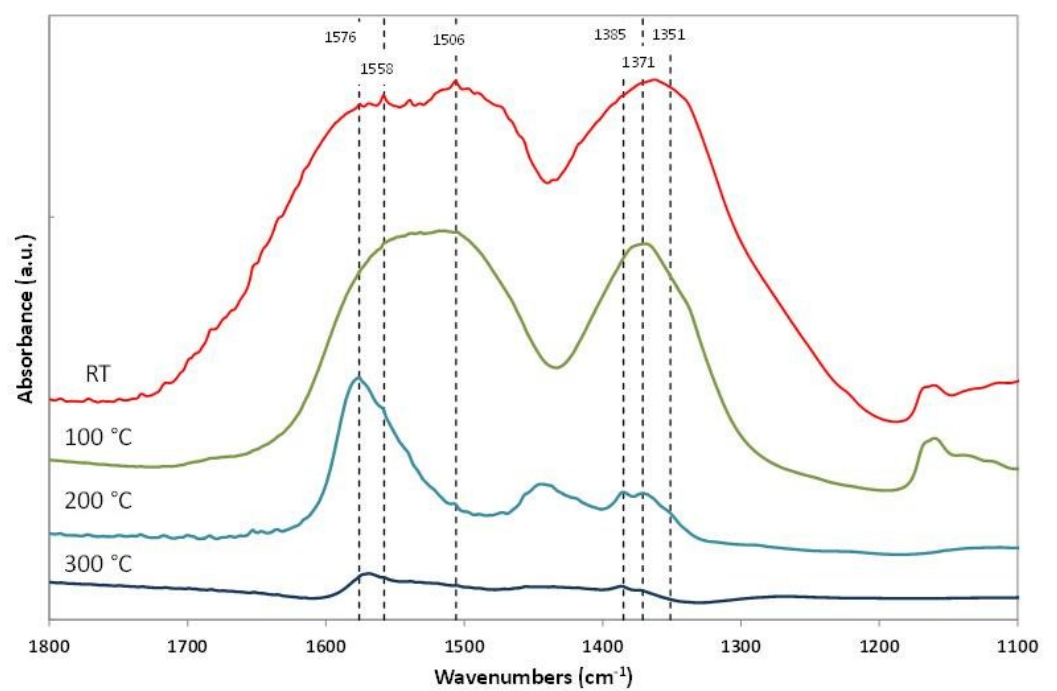


Figure S8. FT-IR of adsorbed CO₂ over CuO/ZrO₂ C

After CO₂ adsorption at RT we obtain a very broad spectrum (Figure S7). After degassing at increasing temperature, three maxima at 1558, 1506 and 1371 cm⁻¹ are detectable that could be due to bicarbonates and carbonates species mainly formed on basic hydroxyl group [69] while two peaks at 1576 and 1351 cm⁻¹, with a spectral gap of 225 cm⁻¹ are diagnostic for bidentate carbonate species on coordinatively unsaturated acid-base pair centers. The bands at 1385 and 1371 cm⁻¹, together to the one at 1576 cm⁻¹, are also indicative for the presence of coordinatively unsaturated O²⁻ centres characterized by high basicity [69, 70]. Therefore the CO₂ adsorption revealed the presence of superficial strongly basic centres and acid-base pairs.

For comparison the spectrum of ZrO₂ C is reported. After evacuation in ultra-high vacuum at 350 °C for one night the material already shows bands due to high-resistant species arising from the contact with atmospheric CO₂ (Figure S8). After CO₂ adsorption and desorption at increasing temperature spectra do not change significantly.

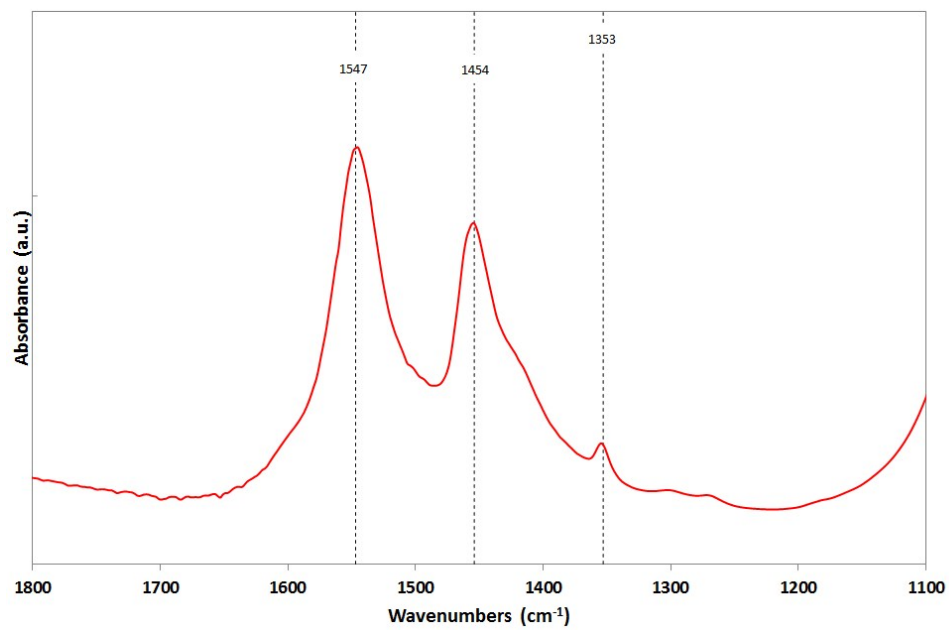


Figure S9. FT-IR of adsorbed CO₂ over ZrO₂ C

Experimental details

All the experiments were performed in duplicate and in triplicate for the best results obtained (that is for experiments 4 and 5 in Table 1 and for the experiments 1 and 6 in Table 2).

Quantitative analysis

Conversion of butanol and **yield** of butylbutanoate were evaluated by GC analysis by using hexadecane as internal standard according to the following formulas:

$$\text{Conv \%} = \left(\frac{\text{Mol butanol } i - \text{mol butanol } f}{\text{mol butanol } i} \right) \times 100$$

$$\text{Mol Butanol } f = \left[\left(\frac{A \text{ butanol}}{A \text{ std}} - b \right) / a \right] \times \text{Mol std}$$

$$Y \% = \left[\frac{\text{Mol butylbutanoate } f}{\text{Mol butanol}/2} \times 100 \right]$$

$$\text{Mol Butylbutanoate} = \left[\left(\frac{A \text{ butylbutanoate}}{A \text{ std}} - b \right) / a \right] \times \text{Mol st}$$

with a and b drawn by the calibration curve.

The **amount of hydrogen** produced has been calculated as follows:

Starting mol of butanol = 0,17 mol

Autoclave dead volume = 100 mL

H₂ pressure produced during reaction = 15 atm

$$\text{mol H}_2 \text{ produced} = \frac{15 \text{ atm} \times 0,1 \text{ L}}{0,082 \left(\frac{\text{atm L}}{\text{mol K}} \right) 298 \text{ K}} = 0,061 \text{ mol}$$

Theoretical mol of H₂ at 40% conv = 0,17 mol × 0,40 = 0,068 mol

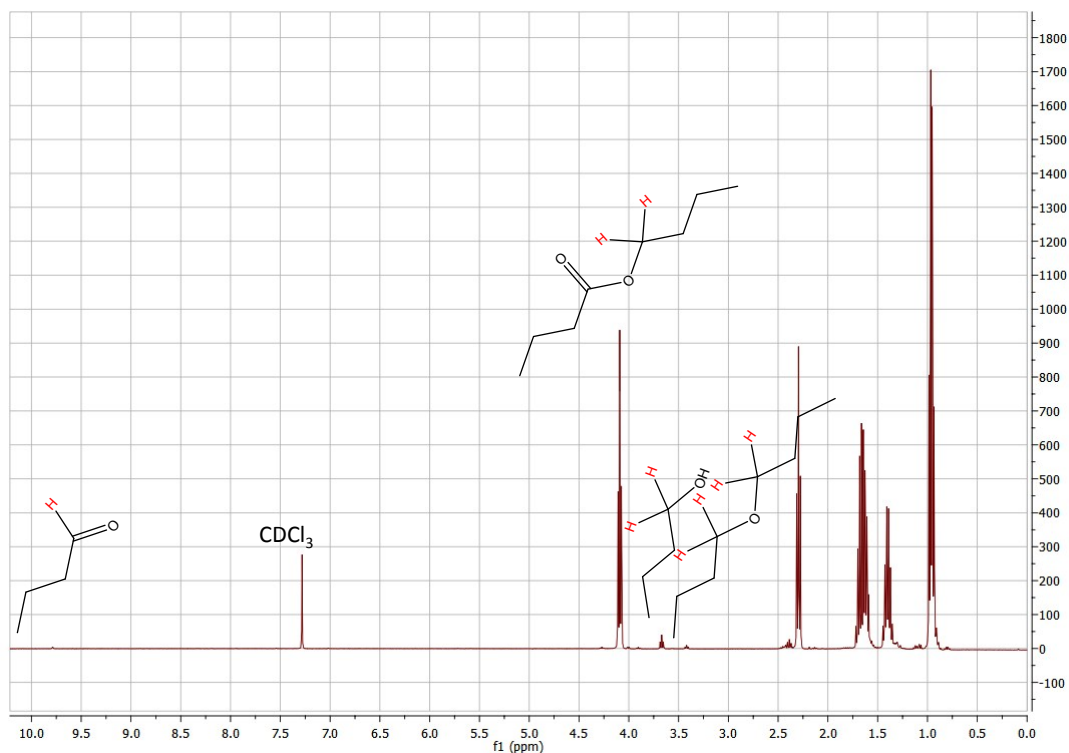


Figure S10. ¹H NMR analysis of reaction mixture obtained from 1-butanol over CuO/ZrO₂ C after 24 h

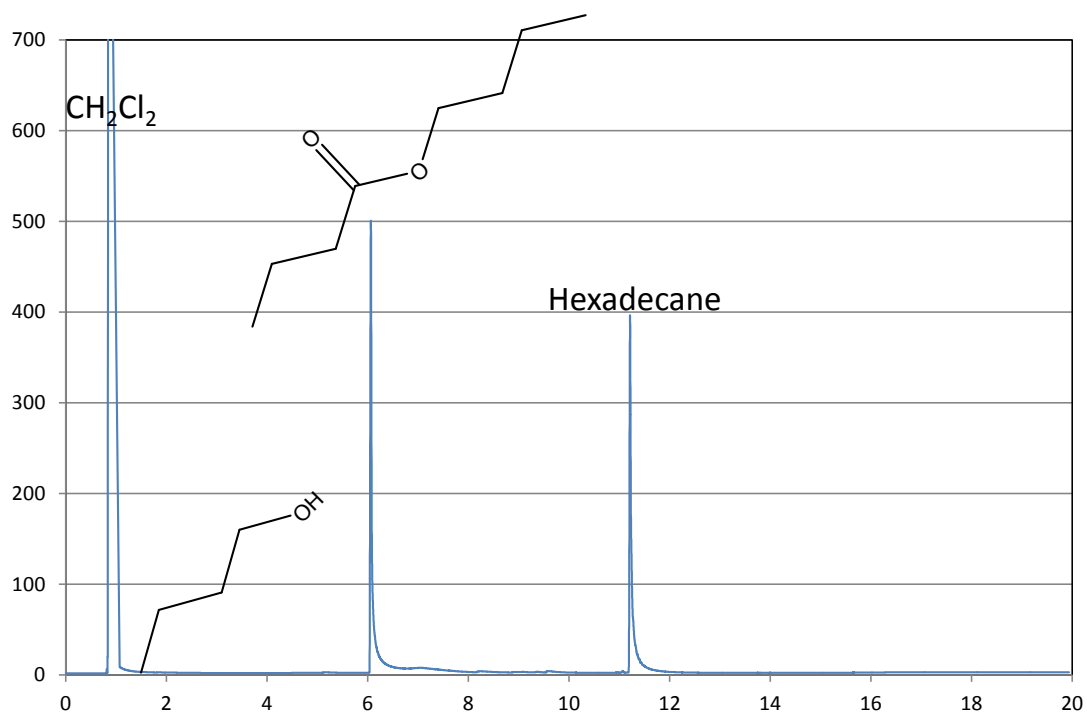


Figure S11. GC-FID analysis of reaction mixture obtained from 1-butanol over CuO/ZrO₂ C after 24 h